

Figure 3. Pseudochelate ring formation between the acetate ester carbonyl group and the coordinated water molecule.

(4) The lanthanide complex formation constants of ligands 2-4 are sometimes greater for the lighter and middle lanthanide ions as compared to those of EDDA (6), even though the protonation constants are smaller for ligands 2-4. This further substantiates the size selectivity of the macrocycles toward the lighter and middle lanthanide ions. On the other hand, the lanthanide complex formation constants of ligand 5 are always greater than the corresponding ones of EDDA (6), despite the facts that the protonation constants of ligand 5 are 2-3 orders of magnitude smaller and both ligands do not possess macrocyclic rings.

This probably can be explained by the possibility of pseudochelate ring formation pictured in Figure 3 between the acetate ester carbonyl groups and coordinated water molecules for Ln-ligand 5 complexes. This kind of pseudochelate ring formation may add additional thermodynamic stability to the complex formation.

In summary, the crown ether-like behavior for lanthanide complexes, i.e., selectivity toward the lighter or middle lanthanide ion, is also seen for macrocyclic ligands with ionizable functional pendant arms in aqueous solution. This seems to be true regardless of where the ionizable functional groups are located in the macrocycle ring. However, with the addition of electron-withdrawing or electron-donating groups, the complexation ability of the macrocyclic ligands can be further modified.

**Acknowledgment.** This material was prepared with the support of U.S. Department of Energy Grant No. DE-FG05-84ER13292; however, any opinions, findings, conclusions, or recommendations expressed herein are those of the authors and do not necessarily reflect the views of DOE.

**Registry No.** 1, 93031-52-8; 2, 93031-53-9; 3, 93031-54-0; 4, 93049-99-1; 5, 17619-53-3; 6, 5657-17-0.

(13) Spirlet, M. R.; Rebizant, J.; Loncin, M. F.; Desreux, J. F. *Inorg. Chem.* **1984**, *23*, 4278-4283.

(14) Desreux, J. F.; Loncin, M. F. *Inorg. Chem.* **1986**, *25*, 69-74.

Contribution from the Monsanto Company,  
Mail Zone Q1B, 800 North Lindbergh Boulevard,  
St. Louis, Missouri 63167

### Convenient Synthesis of and Additional Characterization Data for Vanadyl Hydrogen Phosphate Tetrahydrate

James T. Wroblewski

Received September 18, 1987

In 1985, Leonowicz et al.<sup>1</sup> reported the single-crystal structure of a polymeric oxovanadium(IV) orthophosphate hydrate with empirical formula  $\text{VOHPO}_4 \cdot 4\text{H}_2\text{O}$ . They observed its transformation to  $(\text{VO})_2\text{P}_2\text{O}_7 \cdot 2$  at 773 K and suggested that  $\text{VOHPO}_4 \cdot$

$0.5\text{H}_2\text{O}$  might be formed by elimination of water from the tetrahydrate. In the same month, Garbassi et al.<sup>4</sup> reported a microcrystalline compound (phase P2) with composition and properties similar to  $\text{VOHPO}_4 \cdot 4\text{H}_2\text{O}$ , which they assumed to be  $(\text{VO})_2\text{P}_2\text{O}_7 \cdot 9\text{H}_2\text{O}$ . Earlier, Poloiko and Teterikov<sup>5</sup> reported limited characterization data for a compound with the same empirical formula. In addition, an identical composition was disclosed in a 1984 U.S. Patent,<sup>6</sup> which described a process for the manufacture of maleic anhydride by *n*-butane selective oxidation on VPO catalysts.<sup>7</sup>

As part of a study of vanadium phosphates, various  $\text{VOHPO}_4$  hydrates were prepared as precursors to  $(\text{VO})_2\text{P}_2\text{O}_7$ . In this note, I report a high-yield synthesis of single-phase  $\text{VOHPO}_4 \cdot 4\text{H}_2\text{O}$  and present vibrational spectral, bulk magnetic susceptibility, and thermal data for this compound. A method for the quantitative conversion of this hydrate to  $\text{VOHPO}_4 \cdot 0.5\text{H}_2\text{O}$  is described.

### Experimental Section

**Materials.** Johnson Matthey Puratronic grade  $\text{V}_2\text{O}_5$ , obtained from Alfa, was used as received.  $\text{D}_3\text{PO}_4$  (85% in  $\text{D}_2\text{O}$ ), DI (53% in  $\text{D}_2\text{O}$ ), and  $\text{D}_2\text{O}$  (99.8 atom % D) were obtained from Sigma. All other chemicals were ACS reagent grade from Fisher.

**Instrumentation.** Magnetic susceptibility data were collected from 4 to 300 K by using a George Associates force magnetometer system. The magnetic field gradient was measured by using a National Bureau of Standards cylindrical Pt susceptibility standard. Field intensity was measured with a calibrated Hall probe. GaAs thermometry was used to measure sample temperature, which was controlled to better than  $\pm 0.08$  K from 4.2 to 50 K. Replicate susceptibility measurements of  $\text{HgCo}(\text{NCS})_4$  from 4.2 to 300 K were fit to the Curie-Weiss law with  $C = 2.358 \pm 0.003$  and  $\theta = -1.92 \pm 0.04$  K, in essential agreement with accepted values<sup>8</sup> of  $2.351 \pm 0.001$  and  $-1.86 \pm 0.01$  K, respectively. The magnetic susceptibility of  $[(\text{CH}_3)_2\text{NHCH}_2\text{CH}_2\text{NH}(\text{CH}_3)_2]\text{CuCl}_4$  was also measured from 4.2 to 50 K to give  $C = 0.439$  and  $\theta = -0.15$  K, in close agreement with published values<sup>8</sup> of 0.433 and  $-0.07$  K, respectively ( $N\alpha = -217 \times 10^{-6}$  cgsu and  $\chi_{\text{dia}} = 60 \times 10^{-6}$  cgsu). Susceptibility data were fit to appropriate theoretical expressions by using a local computer program that incorporated the Simplex minimization algorithm.<sup>9</sup> Vacuum desiccation of  $\text{VOHPO}_4 \cdot 4\text{H}_2\text{O}$  during susceptibility measurements was minimized by sealing samples in poly(tetrafluoroethylene) cylinders with threaded closures.

Powder X-ray diffraction patterns were obtained by using a Sintag/Seifert automated powder diffractometer with an EG&G Ortec germanium crystal energy dispersive detector.  $\text{Cu K}\alpha_1$  radiation (154.051 pm) was used to index the patterns. Laser Raman spectra were recorded on a Ramanor U-1000 spectrophotometer at Washington University, St. Louis, MO. The laser (514.532 nm) was operated at 100-mW power. Thermal analysis curves were obtained by using a Mettler TA-1 thermal analyzer.

**Syntheses.  $\text{VOHPO}_4 \cdot 4\text{H}_2\text{O}$ .** *Caution!* This synthesis liberates iodine vapor. All operations should be conducted in a hood.

A mixture of 85%  $\text{H}_3\text{PO}_4$  (28 g) and  $\text{V}_2\text{O}_5$  (20 g) in distilled water (70 mL) was stirred at 80 °C for 30 min to give the hydrate of  $\text{VOPO}_4$ . This mixture was heated to 90 °C and treated dropwise with 57% aqueous HI (50 g). After this addition, the mixture was stirred at 90 °C for 1 h. Water was added to maintain a volume of 150 mL. The product mixture was suction filtered to remove  $\text{I}_2$ . The dark green filtrate was boiled with a subsurface  $\text{N}_2$  purge until  $\text{I}_2$  evolution ceased. The dark blue solution was diluted to 150 mL, filtered, and stirred at room temperature for 20 h to precipitate a blue solid. The solid was collected,

(2) A single-crystal X-ray structure of  $(\text{VO})_2\text{P}_2\text{O}_7$  has been published: Gorbunova, Yu. E.; Linde, S. A. *Dokl. Akad. Nauk SSSR* **1978**, *245*, 584-588; *Sov. Phys.—Dokl. (Engl. Transl.)* **1979**, *24*, 138-140.

(3) Single-crystal X-ray structures of  $\text{VOHPO}_4 \cdot 0.5\text{H}_2\text{O}$  have been published in ref 1 and the following references: (a) Torardi, C. C.; Calabrese, J. C. *Inorg. Chem.* **1984**, *23*, 1308-1310. (b) Johnson, J. W.; Johnston, D. C.; Jacobson, R. J.; Brody, J. F. *J. Am. Chem. Soc.* **1984**, *106*, 8123-8128.

(4) Garbassi, F.; Bart, J. C. J.; Montino, F.; Petri, G. *Appl. Catal.* **1985**, *16*, 271-287.

(5) Poloiko, V. I.; Teterikov, R. I. *Zh. Neorg. Khim.* **1981**, *26*, 2972-2976; *Russ. J. Inorg. Chem. (Engl. Transl.)* **1981**, *26*, 1589-1592.

(6) Mount, R. A.; Wroblewski, J. T. U.S. Patent 4448 978, 1984.

(7) For a recent review of VPO catalysis, see: Hodnett, B. K. *Catal. Rev.—Sci. Eng.* **1985**, *27*, 373-424.

(8) Brown, D. B.; Crawford, V. H.; Hall, J. W.; Hatfield, W. E. *J. Phys. Chem.* **1977**, *81*, 1303-1306.

(9) Deming, S. N.; Morgan, S. L. *Anal. Chem.* **1973**, *45*, 278A.

(1) Leonowicz, M. E.; Johnson, J. W.; Brody, J. F.; Shannon, H. F., Jr.; Newsam, J. M. *J. Solid State Chem.* **1985**, *56*, 370-378.

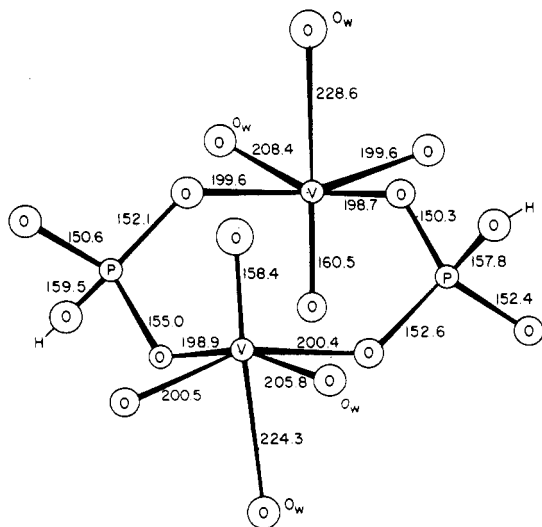


Figure 1. Basic structural element of  $\text{VOHPO}_4 \cdot 4\text{H}_2\text{O}$  (bond distances in pm) as determined by Leonowicz et al.<sup>1</sup>

washed with acetone, and air-dried at room temperature. The average yield of  $\text{VOHPO}_4 \cdot 4\text{H}_2\text{O}$  from six preparations was 92.5%. The D-substituted compound was prepared as above except that 54 g of 53% DI in  $\text{D}_2\text{O}$  was used as the reductant. All samples gave required elemental analyses.

$\text{VOHPO}_4 \cdot 4\text{H}_2\text{O}$ , as prepared by the aqueous HI reduction method, was soluble in methanol and ethanol. Attempted recrystallization of the tetrahydrate by slow evaporation of the alcohol solvent gave an amorphous product. Rapid precipitation from solution by water or acetone addition gave a mixture of microcrystalline  $\text{VOHPO}_4 \cdot 4\text{H}_2\text{O}$  and amorphous material.

$\text{VOHPO}_4 \cdot 0.5\text{H}_2\text{O}$ . A dark gray solid was obtained by heating  $\text{VOHPO}_4 \cdot 4\text{H}_2\text{O}$  in air at 125 °C for 16 h (15.8 ± 0.5% weight loss, average of six preparations). A mixture of this gray solid (260 g) and distilled water (600 mL) was heated to 150 °C in a sealed, stainless-steel autoclave. The stirred mixture was held at this temperature (±5 °C) for 4 h. After cooling, the product mixture was dried in air at 125 °C for 16 h to give  $\text{VOHPO}_4 \cdot 0.5\text{H}_2\text{O}$  in 96% yield. This product was characterized by comparing its powder X-ray diffraction pattern (Table SI, supplementary material), chemical analysis, and infrared spectrum to that of authentic hemihydrate.<sup>3</sup>

A direct conversion of  $\text{VOHPO}_4 \cdot 4\text{H}_2\text{O}$  to  $\text{VOHPO}_4 \cdot 0.5\text{H}_2\text{O}$ , without intermediate partial dehydration, was not observed with the conditions above: Unreacted  $\text{VOHPO}_4 \cdot 4\text{H}_2\text{O}$  and an uncharacterized vanadium phosphate hydrate were obtained. In addition, various other conditions of temperature, pressure, concentration, and time failed to give the hemihydrate directly from the tetrahydrate.

## Results and Discussion

The structure<sup>1</sup> of  $\text{VOHPO}_4 \cdot 4\text{H}_2\text{O}$  coordination polymer is composed of the two-vanadium unit shown in Figure 1. These dimers are connected by bridging monohydrogen phosphate groups to form a double chain of  $\text{PO}_4$  tetrahedra and  $\text{VO}_6$  octahedra that is parallel to the *a* crystallographic direction. Two water molecules,  $\text{O}_w$ , are coordinated to vanadium. The other water molecules are held in the lattice through a series of rather complex hydrogen-bonding networks.

X-ray powder diffraction patterns of  $\text{VOHPO}_4 \cdot 4\text{H}_2\text{O}$  samples made by the aqueous HI method are indexed with unit cell parameters  $a = 637.9$  pm,  $b = 892.1$  pm,  $c = 1346.2$  pm,  $\alpha = 79.95^\circ$ ,  $\beta = 76.33^\circ$ , and  $\gamma = 71.03^\circ$ .<sup>1</sup> Observed and calculated *d* spacings for a freshly ground, representative preparation of  $\text{VOHPO}_4 \cdot 4\text{H}_2\text{O}$  are given in Table SII (supplementary material). Of 68 observed reflections below 45° in  $2\theta$ , only one weak reflection at  $d = 6.722$  Å is not indexed with these unit cell parameters. Ground samples of this compound change color from blue to green after several days exposure to ambient air. This color change is accompanied by a change in the relative intensity of the 011 and 002 reflections.

Room-temperature IR and laser Raman spectra of  $\text{VOHP} \cdot 4\text{H}_2\text{O}$  are shown in Figure 2. The envelope of O–H stretching absorptions, centered at about 3400  $\text{cm}^{-1}$ , is composed of at least three bands at 3520, 3370, and 3040  $\text{cm}^{-1}$ . Substitution of H with D shifts these absorptions to 2590, 2490, and 2320  $\text{cm}^{-1}$ , respectively. Likewise, the H–O–H bending mode at 1640  $\text{cm}^{-1}$  in  $\text{VOHPO}_4 \cdot 4\text{H}_2\text{O}$  moves to 1500  $\text{cm}^{-1}$  in  $\text{VODPO}_4 \cdot 4\text{D}_2\text{O}$ . The convolution of absorptions centered at about 1100  $\text{cm}^{-1}$  contains  $\text{PO}_4$  and  $\text{V}=\text{O}$  vibrations. Although a sharp absorption at 987  $\text{cm}^{-1}$  was assigned<sup>4</sup> to the  $\text{V}=\text{O}$  stretch, considerable overlap of bands in this region in the IR make this assignment doubtful. A laser Raman spectrum (Figure 2 insert) of  $\text{VOHPO}_4 \cdot 4\text{H}_2\text{O}$  shows prominent absorptions at 1080, 998, and 982  $\text{cm}^{-1}$  that are assigned to  $\nu_1(\text{PO}_4)$ ,  $\nu(\text{V}=\text{O})$ , and  $\nu_3(\text{PO}_4)$ , respectively.

Weight loss and DTA curves for  $\text{VOHPO}_4 \cdot 4\text{H}_2\text{O}$  are shown in Figure 3. The weight loss curve is interpreted in terms of two processes: loss of lattice and coordinated water below about 180 °C and loss of water by condensation of  $\text{HPO}_4^{2-}$  groups from 400 to about 600 °C. Separate processes due to loss of lattice water and loss of coordinated water are not observed in this experiment. In static, inert-atmosphere heating experiments, X-ray amorphous phases with variable composition are obtained below 600 °C.  $\text{VOHPO}_4 \cdot 0.5\text{H}_2\text{O}$  is not observed as a crystalline phase in these experiments. A nondiffracting phase with composition  $\text{V}_2\text{P}_2\text{O}_9$  is prepared by heating a sample of the tetrahydrate in flowing Ar at 650 °C for 15 min. When the same experiment is conducted at 800 °C, a sample of well-crystallized  $(\text{VO})_2\text{P}_2\text{O}_7$  is obtained.

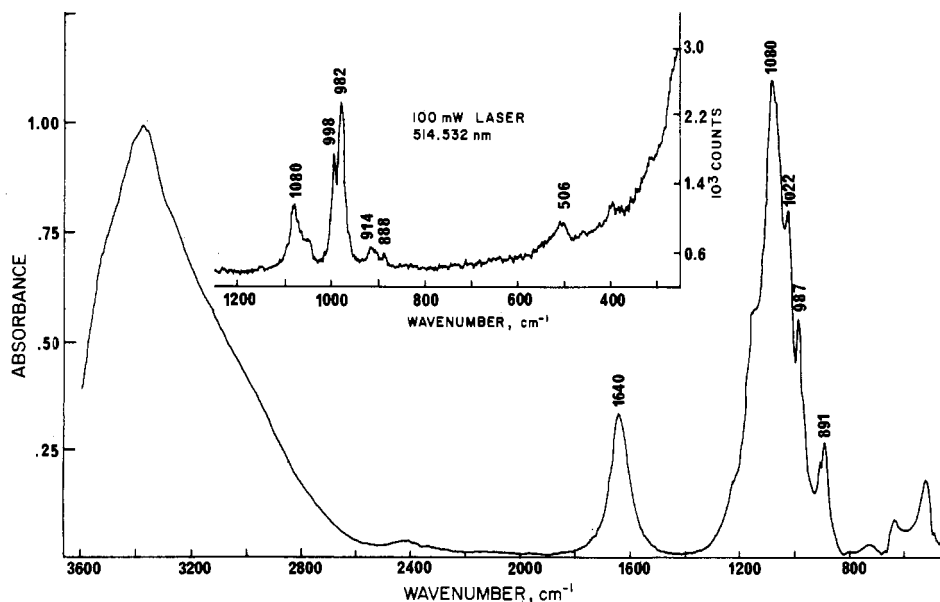
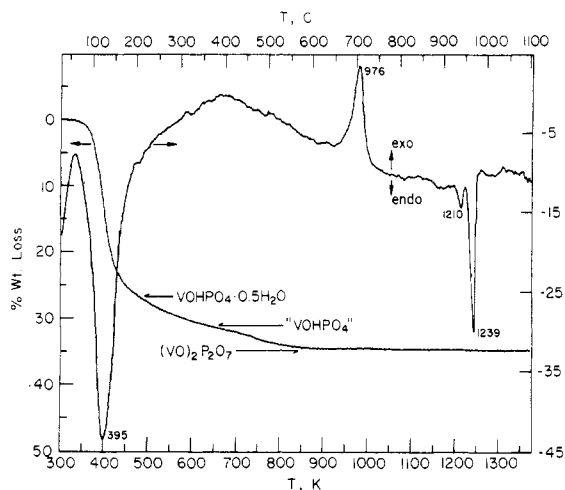
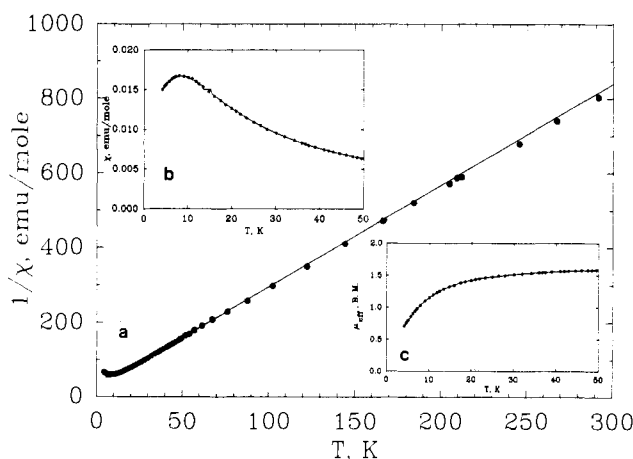


Figure 2. KBr matrix infrared and laser Raman (insert) room-temperature spectra of  $\text{VOHPO}_4 \cdot 4\text{H}_2\text{O}$ .



**Figure 3.** Thermal analysis curves (weight loss and DTA) for  $\text{VOHPO}_4 \cdot 4\text{H}_2\text{O}$  obtained in flowing He at  $10^\circ\text{C}/\text{min}$  heating rate.



**Figure 4.** Magnetic susceptibility data for polycrystalline  $\text{VOHPO}_4 \cdot 4\text{H}_2\text{O}$ : (a) inverse susceptibility vs  $T$  (4–300 K); (b) susceptibility vs  $T$  (4–50 K); (c) effective magnetic moment vs  $T$  (4–50 K). The smooth curves represent a fit to the Bonner and Fisher linear-chain model, eq 1, with  $J = -4.5 \text{ cm}^{-1}$  and  $g = 1.98$ .

These experiments suggest that the exotherm near  $700^\circ\text{C}$  is associated with crystallization of an amorphous precursor to vanadyl diphosphate. The sharp endothermic peak at  $1239 \text{ K}$  corresponds to the melting point of authentic  $(\text{VO})_2\text{P}_2\text{O}_7$ .<sup>10</sup> A small endothermic feature at about  $1210 \text{ K}$  is associated with the melting temperature of  $\text{V}^{\text{III}}_2(\text{VO}^{2+})(\text{P}_2\text{O}_7)_2$ .<sup>11</sup>

Magnetic susceptibility data, obtained at  $6 \text{ kOe}$  and corrected for ligand diamagnetism ( $-95 \times 10^{-6} \text{ cgsu}$ ), for polycrystalline  $\text{VOHPO}_4 \cdot 4\text{H}_2\text{O}$ , are shown in Figure 4. A plot of inverse corrected susceptibility vs temperature (Figure 4a) is linear above  $25 \text{ K}$ . The susceptibility curve (Figure 4b) has a broad maximum at about  $8 \text{ K}$ . The effective magnetic moment (Figure 4c) decreases from  $1.78 \mu_{\text{B}}$  at about  $300 \text{ K}$  to  $0.75 \mu_{\text{B}}$  at  $4.2 \text{ K}$ . Attempts to fit these data to the HDVV exchange coupled dimer model gave unacceptable values of  $J$  and  $g$ . A better fit, shown in Figure 4, is obtained by using a numerical representation<sup>12</sup> (eq 1, where  $x = |J|/kT$ ) of the Bonner and Fisher  $S = 1/2$  linear-chain model<sup>13</sup>

$$\chi_{\text{M}} = (Ng^2\mu_{\text{B}}^2/kT)(0.25 + 0.14995x + 0.30094x^2) / (1.0 + 1.9862x + 0.68854x^2 + 6.0626x^3)^{-1} \quad (1)$$

(10) Wroblewski, J. T., unpublished observation.

(11) The compound  $\text{V}^{\text{III}}_2\text{VO}(\text{P}_2\text{O}_7)_2$  was prepared by reaction of  $\text{VOHPO}_4 \cdot 4\text{H}_2\text{O}$  with water-saturated  $\text{N}_2$  at  $1100^\circ\text{C}$ . The single-crystal structure of this mixed-valent trimer has been determined: Wroblewski, J. T.; Thompson, M. R., manuscript in preparation.

(12) Hall, J. W. Ph.D. Dissertation, The University of North Carolina at Chapel Hill, 1977.

(13) Bonner, J.; Fisher, M. E. *Phys. Rev. A* **1964**, *135*, 640–658.

with the Hamiltonian in eq 2. Best fit parameters are  $J = 4.5$

$$H = -2J\sum(\text{S}_i^z\text{S}_{i+1}^z + \text{S}_i^x\text{S}_{i+1}^x + \text{S}_i^y\text{S}_{i+1}^y) \quad (2)$$

$\text{cm}^{-1}$  and  $g = 1.98$ . Paramagnetic impurity and interchain exchange corrections to eq 1 are unnecessary within experimental uncertainty.

The experimental results for  $\text{VOHPO}_4 \cdot 4\text{H}_2\text{O}$  described above are consistent with the single-crystal structure of Leonowicz et al.<sup>1</sup> Repeated attempts to isolate  $\text{VOHPO}_4 \cdot 0.5\text{H}_2\text{O}$  as an intermediate in the  $\text{VOHPO}_4 \cdot 4\text{H}_2\text{O}$  to  $(\text{VO})_2\text{P}_2\text{O}_7$  transformation were unsuccessful:  $\text{VOHPO}_4 \cdot 0.5\text{H}_2\text{O}$  could only be obtained by dehydration of the tetrahydrate to an amorphous vanadium phosphate followed by hydrothermal reaction (Experimental Section). Thus, although the structures of  $\text{VOHPO}_4 \cdot 4\text{H}_2\text{O}$ ,  $\text{VOHPO}_4 \cdot 0.5\text{H}_2\text{O}$ , and  $(\text{VO})_2\text{P}_2\text{O}_7$  are related, there is no direct evidence to support the intermediacy of the hemihydrate in the solid-state decomposition of the tetrahydrate to the diphosphate.

**Acknowledgment.** Powder X-ray diffraction patterns were obtained by Frank L. May. John J. Freeman collected Raman and IR spectral data. Thermal analyses were performed by Deborah A. Carter.

**Supplementary Material Available:** Tables of observed and calculated X-ray powder diffraction data for  $\text{VOHPO}_4 \cdot 4\text{H}_2\text{O}$  and  $\text{VOHPO}_4 \cdot 0.5\text{H}_2\text{O}$  (3 pages). Ordering information is given on any current masthead page.

Contribution from the Departments of Inorganic Chemistry, University of Nijmegen, Toernooiveld, 6525 ED Nijmegen, The Netherlands, and University of Minnesota, Minneapolis, Minnesota 55455

#### Separation of Cationic Metal Cluster Compounds by Reversed-Phase HPLC

Wim Bos,<sup>†</sup> J. J. Steggerda,<sup>\*†</sup> Shiping Yan,<sup>‡§</sup> Joseph A. Casalnuovo,<sup>†</sup> Ann M. Mueting,<sup>†</sup> and Louis H. Pignolet<sup>\*†</sup>

Received September 3, 1987

High-performance liquid chromatography (HPLC)<sup>1</sup> has been used as a standard technique in organic chemistry for many years. It has only been in the last few years, however, that HPLC has been recognized to be equally useful in inorganic chemistry. A number of HPLC separations of neutral mononuclear compounds or cluster compounds have been reported.<sup>2–7</sup> For the separation of mononuclear cationic complexes, new techniques such as ion-pairing chromatography have been introduced.<sup>8–13</sup> No standard methods, however, have been developed for the separation of cationic metal cluster compounds. Because our research groups have been synthesizing a wide variety of cationic metal clusters in the last few years,<sup>14–23</sup> we have begun to utilize HPLC for the separation and identification of these compounds. A wide variety of large cationic metal cluster compounds have been successfully separated by this technique. In this report we present some of our achievements in this area.

#### Experimental Section

Gold cluster compounds were prepared according to the literature.<sup>24–30</sup> The osmium-gold,<sup>31</sup> ruthenium-gold,<sup>21,23</sup> rhenium-gold,<sup>20,22</sup> and platinum-gold<sup>20,32,33</sup> clusters were obtained by procedures previously described.

**Gold Cluster Compounds.** The HPLC separations were performed with a modular LKB liquid chromatographic system consisting of a 2150 HPLC pump, 2152 controller, 2158 Uvicord SD detector operated at 254

<sup>†</sup> University of Nijmegen.

<sup>‡</sup> University of Minnesota.

<sup>§</sup> Visiting scientist from Nankai University of Tianjin, China.